



Vanadium loaded carbon-based monoliths for the on-board NO reduction: Influence of vanadia and tungsten loadings

M.J. Lázaro^{a,*}, A. Boyano^a, C. Herrera^b, M.A. Larrubia^b, L.J. Alemany^b, R. Moliner^a

^a Instituto de Carboquímica CSIC, Miguel Luesma Castan 4, Zaragoza 50.018, Spain

^b Departamento de Ingeniería Química, Facultad de Ciencias, Campus de Teatinos s/s, Universidad de Málaga, E-29071 Malaga, Spain

ARTICLE INFO

Article history:

Received 4 February 2009

Received in revised form 23 June 2009

Accepted 25 June 2009

Keywords:

Vanadia
Tungsten
SCR-NH₃
Carbon-based catalyst
On-board NO reduction

ABSTRACT

Carbon-coated catalysts doped with tungsten and vanadia oxides with different V and W loadings have been prepared by the ionic exchange method and characterized. The surface, structure and composition have been investigated by XPS, Raman, N₂ sorption at 77 K, TPD-NH₃ and reactivity tests for the SCR of NO with NH₃ at low temperatures. Under reaction conditions, NO conversions were found to go through a maximum with vanadia surface coverage at approximately half a monolayer. The observed decrease in the SCR activity at higher vanadia loadings can be attributed to either a loss of dispersion or loss of textural properties. Maximum NO conversion is ascribed to the higher Brønsted proton acidity (V⁴⁺) of the centres that decreases with increasing vanadia loadings up to 3 wt% loading due to the increase of V⁴⁺/V⁵⁺ ratio.

Large amounts of tungsten (5%, w/w) upon or before addition of vanadia do not provide an enhancement of activity. The results indicate that W addition increases surface acidity leading to stronger Brønsted or even Lewis acid centre creation.

© 2009 Elsevier B.V. All rights reserved.

1. Introduction

The proven technological options available to abate NO_x emissions from combustion gasses from current engines are essentially two. In the case of lean burn engines, three-way catalysts are not effective due to the excess of air [1] and consequently a new technology should be developed. These emissions have a high presence of oxygen that is similar to NO_x emissions from stationary sources. Consequently, the developed technology used in stationary sources can be successfully adapted to on-board applications. To deal with NO_x emissions from stationary sources in the presence of an excess of oxygen, the reduction with ammonia using V₂O₅/TiO₂ or metal-zeolites [2] is the route of choice.

In the recent past, SCR of NO by urea has become a point of interest for automotive applications due to the high activity of V₂O₅/TiO₂ catalyst for NO reduction in lean conditions such as diesel exhausted gas [3]. However, these catalysts present two critical problems due to the differences between the catalyst and diesel engine operation conditions, which should be solved before their application: the temperature range and the deactivation by SO₂. Moreover, not only is V₂O₅ the active reaction site for the reduction of NO_x, but also for the oxidation of SO₂ to SO₃. Promoters including tungsten and molybdenum have been added to V₂O₅/TiO₂ catalysts

to improve the thermal stability due to the retardation of anatase to rutile phase transition and reducing the activity of SO₂ oxidation.

Tungsten is usually added in high amounts (around 10 wt%) comparing to V₂O₅ (around 1 wt%). Several studies [4,5] have shown that the catalytic properties as well as the chemical and physical structure of such products are markedly influenced by parameters, such as the method of preparation, the concentration of the active component and the nature of the supports. According to them, tungsten addition to V₂O₅/TiO₂ under monolayer coverage is able to reduce its activity for SO₂ oxidation [6], to widen the temperature window, to enhance poison resistance towards alkali oxides, to lower the ammonia oxidation activity of the catalysts and finally not only to generate new acid sites but also to increase the Brønsted acidity.

The formation of new acid sites when two oxides are mixed has been discussed in detail in the literature; and, in fact, models have been proposed for predicting these new acid sites [7]. The generation of new acid sites by mixing two oxides on the surface phase (on a support) has been discussed elsewhere [8]. The acid site formation by the combination of TiO₂ and WO₃, in particular, was studied by Yamaguchi et al. [9] and explained by a model in which an excess of positive charge from tungsten in the mixed oxide structure would produce Lewis acid sites. Water molecules (either from the SCR product or the reactant gas) can be chemisorbed on the Lewis acid sites to produce Brønsted acid sites that are active sites and enhance SCR activity [10]. Therefore the role of WO₃ in the commercial catalysts is the stabilization the Brønsted acidity.

* Corresponding author. Tel.: +34 976733977; fax: +34 976733318.
E-mail address: mlazaro@icb.csic.es (M.J. Lázaro).

Table 1
Description of the carbon-based catalysts prepared.

Carbon-based catalyst	Short description
Support	Oxidized HNO ₃ (1N) for 24 h carbon-coated monolith
NH ₄ VO ₃ (1%V)	Support doped with 1 wt% V from NH ₄ VO ₃
NH ₄ VO ₃ (3%V)	Support doped with 3 wt% V from NH ₄ VO ₃
NH ₄ VO ₃ (5%V)	Support doped with 5 wt% V from NH ₄ VO ₃
V ₂ O ₅ (1%V)	Support doped with 1 wt% V from V ₂ O ₅
V ₂ O ₅ (3%V)	Support doped with 3 wt% V from V ₂ O ₅
V ₂ O ₅ (5%V)	Support doped with 5 wt% V from V ₂ O ₅
5% W	Support doped with 5 wt% W from (NH ₄) ₆ W ₁₉ O ₃₆ ·xH ₂ O
3% V–5% W	Support doped firstly with 3% V from NH ₄ VO ₃ and subsequently with 5 wt% W from (NH ₄) ₆ W ₁₉ O ₃₆ ·xH ₂ O
5% W–3% V	Support doped firstly with 5 wt% W from (NH ₄) ₆ W ₁₉ O ₃₆ ·xH ₂ O and subsequently with 3% V from NH ₄ VO ₃
3% V–5% W simultaneously	Support doped simultaneously with 3% V from NH ₄ VO ₃ and 5 wt% W from (NH ₄) ₆ W ₁₉ O ₃₆ ·xH ₂ O

One type of catalysts that fulfils the two above commented requirements for on-board installation is the carbonaceous catalysts. Carbonaceous catalysts are known to be stable under basic and acid conditions, have a good performance for the SCR-NH₃ at lower temperatures, a good resistance to SO₂ and a good adhesion of carbon coating to the cordierite to withstand attrition phenomena [11–18,29–32]. These characteristics are an advantage in comparison to commercial catalysts mostly based on metallic oxide [33].

In this work, carbon-based cordierite monoliths have been prepared and tested in the SCR-NH₃ reduction simulating on-board diesel conditions. Carbon supports can be modulated reaching different surface chemistry and textural properties depending on the preparation process and especially on both the oxidation and activation process as reported in detail somewhere else [12]. The influence of vanadium and tungsten loading will be investigated herein. As previously commented, tungsten is a popular promoter of commercial catalysts; however, there are not systematic studies above its effect on carbon-based catalysts since the study of vanadia loading in carbon-based catalytic activity for the SCR reaction has been poorly investigated. García-Bordejé et al. [30] reported the SCR activity increases as long as vanadia loading increase to a certain extent. Once monolayer coverage is reached, the highest vanadia loadings produce crystallites decreasing total vanadia area exposed to reaction gasses and consequently decreasing SCR activity.

2. Experimental

2.1. Catalyst preparation

Cordierite monoliths were coated with a carbon layer by means of the dip-coating method as described in detail elsewhere [13]. Briefly, it consists in dipping the cordierite monolith (400 cps, 1 cm diameter and 5 cm length) into a liquid polymer that is subsequently cross-linked and carbonised. To coat the monoliths two carbon precursors were used polyethylene-glycol 6000 mol wt (Sigma-Aldrich) (PEG) and Furan resin (Huttene-Albertus). The first is in liquid state and the latter is solid ground in a mill and sieved to diameter lower than 100 m. The dip-coating was carried out with mixtures of Furan resin, PEG, acetone and HNO₃ as polymerisation catalysts, after withdrawing the monoliths from the blend; they were flushed with pressurized air to remove the excess of liquid in the channels. The polymer-coated monoliths were cured at room temperature overnight and for 12 h at 108 °C. Carbonisation of the coated monoliths was carried out in a stainless steel reactor for 4 h at 700 °C in a flow of Argon. Afterwards, they were activated with CO₂ at 900 °C for 4 h and treated for 24 h with HNO₃ 1N at room temperature to created oxygen superficial groups. These conditions have been established in a previous work [14].

The as-prepared carbon-coated monoliths were loaded with vanadium 1, 3 or 5 wt% and in some cases with tungsten 5 wt% of

carbon coatings. The impregnation was carried out by ion-exchange with a solution of either NH₄VO₃ or V₂O₅ or (NH₄)₆W₁₉O₃₆·xH₂O. The amount of precursor in the suspension in distilled water was calculated as the stoichiometric amount to get the desired vanadium or tungsten loading on carbon as described in [14]. The solution was stirred for 18 h and after this process the monoliths were rinsed with distilled water in the same setup. After drying the monoliths first at room temperature overnight and later 2 h at 110 °C, the catalyst was calcined in Ar at 350 °C. The order of vanadia and tungsten impregnation was altered to be aware of the influence of the preparation method on the activity. Although real concentrations of the as-prepared catalysts were not measured in this work, real concentrations of catalysts prepared in the same way were measured and reported previously in [14,30,34] and of similar carbon-based catalysts in [35]. According to these data the real and nominal concentration of the catalyst is really close and therefore we have the assumption that the as-prepared catalysts have close values of real and nominal concentrations of active phase. Table 1 shows a short description of the as-prepared catalysts.

2.2. Catalytic activity

The activity tests were carried out in a quartz reactor with a gas containing of 1000 ppmv NO, 1000 ppmv NH₃ and 10% O₂ (v/v) an Argon to balance at 150, 250 and 350 °C and a space velocity of around 34,000 h⁻¹. The gases were dosed by means of mass flow meters and fed to the cylindrical quartz reactor heated by an electric oven. The concentrations of NO, NH₃, O₂, N₂ and N₂O in the outlet gases were continuously measured in a mass spectrometer (Balzers 422) connected on-line. The mass spectrometer was calibrated using cylinders of known concentration. The percentage of NO reduction and the selectivity towards N₂ were calculated as follows:

$$\% \text{NO conversion} = 100 \times \frac{C_{\text{NO}}^i - C_{\text{NO}}}{C_{\text{NO}}^i} \quad (1)$$

$$\% \text{Selectivity toward N}_2 = 100 \times \frac{C_{\text{N}_2} - C_{\text{N}_2}^i}{[(C_{\text{N}_2} - C_{\text{N}_2}^i) + (C_{\text{N}_2\text{O}} - C_{\text{N}_2\text{O}}^i)]} \quad (2)$$

where C_{NO}^i , $C_{\text{N}_2}^i$ and $C_{\text{N}_2\text{O}}^i$ are the measured initial concentrations of NO, N₂ and N₂O, respectively, and C_{NO} , C_{N_2} , $C_{\text{N}_2\text{O}}$ the concentrations of those gases once the steady state is reached.

Runs have been repeated in a random order. Results presented in the graphics correspond to the average NO conversion under each operation conditions. Statistical parameters (standard deviation variance and confidence level) have also been calculated for each experimental set. The lowest confidence value obtained in the experimental runs is 85% although most of the series shown a confidence value around 90%.

2.3. Catalyst characterization

Doped catalysts were physically and chemically characterized by means of different techniques and methods:

- *Nitrogen adsorption isotherms at 77 K* were obtained in a Micromeritics ASAP 2020 unit. Prior to tests, the samples were out gassed at 200 °C up to a steady vacuum of 1×10^{-6} Torr was achieved. The specific surface area (SSA) was calculated applying the Brunauer–Emmett–Teller (BET) equation to these isotherms. Empirical *t*-plot method was used for the calculation of micro-pore volume. Mesopore volume was calculated by means of BJH method.
- *Temperature-programmed adsorption* was performed using 0.6 g of sample placed inside quartz U-tube, under a stream of NH₃ flowing through at 30 ml/min. The sample was heated up by an electric oven to a temperature of 1050 °C, at a heating rate of 10 °C/min. The gases evolved with each increase of 100 °C were stored in special bags and further analyzed by gas chromatography (Porapak Q and molecular sieve 13× columns) to determine the amounts of CO and CO₂ desorbed. This method has become rather popular among the different techniques used to characterize the functional groups on carbon surface [15,16]. The surface chemistry of a carbon material is basically determined by the acidic and basic character of its functionalities such as carboxyls, lactones and phenols while pyrones, chromenes, ethers and carbonyls are responsible for basic properties on carbon surfaces [17,18]. Although there is not a total agreement in literature with respect to the TPD peaks assignment to specific surface groups, some general trends can be established: CO₂ peaks result from carboxylic acids at low temperatures or lactones at higher temperatures, carboxylic anhydrides originate both CO and CO₂, and phenols, ethers, carbonyls and quinones evolve mainly as CO.
- *Ammonia chemisorption* was carried out in a Micromeritics Pulse Chemisorb 2700 apparatus. The samples of 200–300 mg were dried before carrying out the chemisorptions at the same temperature around 20 min. Prior to the TPD-NH₃ runs, samples were subjected for 30 min to a flow of 30 ml/min of He at 150 °C. Chemisorptions were performed injecting pulses of 108 μl of pure ammonia, and measuring the amount of ammonia consumed by means of a thermal conductivity detector. Ammonia is a basic molecule that is desorbed either on Brønsted acid sites through the formation of NH₄⁺ ion or in Lewis acid sites through coordinative complexation.
- *Raman spectra* were recorded on a Bruker-Senterra Raman imager microscope with the 532 nm Nd–YAG laser and a CCD detector. Raman frequency was calibrated by a silicon slide. The laser was focused on the solid samples which were dispersed on microscope slides. Each spectrum was collected at room temperature under 10 mW of laser power. The experiments were performed in a dark environment to avoid interference from light and cosmic radiation.
- *Transmission Electron Microscopy (TEM)* images were taken with a Philips CM200 (200 kV) microscope equipped with an EDX (Energy Dispersive X-ray) detector on powder sample deposited onto a copper mesh grid with a carbon film.
- *Finally, X-ray Spectroscopy (XPS)* for the internal plates of monolith were acquired with a Physical Electronic 5700 spectrometer equipped with a hemispherical electron analyser and Mg Kα X-ray exciting source (1253.6 eV, 15 kV, 300 W). Samples were placed under vacuum (10⁻⁹ Torr) and time of irradiation was minimized to avoid the metals reduction. It has been used as an internal patron for calibration Al 2p (73.9 eV) considering a deviation ±0.2 eV. As a consequence of the asymmetry presented by the signals, the bands are the result of the contribution of more than one species and the relative population have been determined by

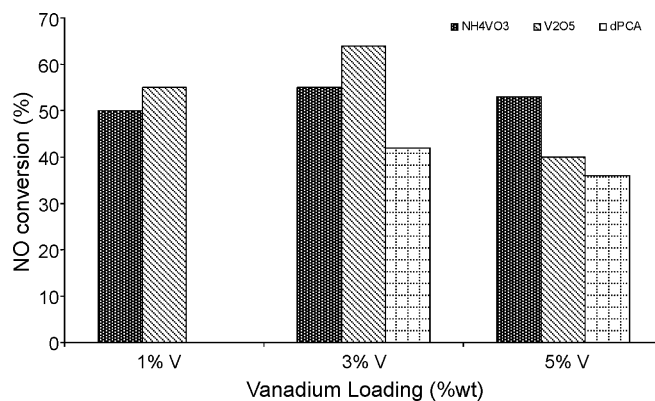


Fig. 1. NO conversion (%) depending on the vanadium loaded and precursor nature.

deconvolution. A strategy was developed for the mathematical deconvolution; in all cases the signal was adjusted to a mathematical response consistent of a Gaussian–Lorentzian distribution (80–20%, respectively) with a minimal χ^2 deviation.

3. Results and discussion

3.1. Effect of vanadia loading

The activity of carbon-based catalysts of variable vanadia loading was determined at three temperatures. Experiments were conducted in the presence of equimolar amounts of NO and NH₃ and excess of O₂. Each catalyst was tested under 150 °C, with the results reported in Fig. 1 and under 150, 200, 250, 300 and 350 °C with the results reported in Fig. 2.

The results in Fig. 1 shows that activity increases with the vanadia loading, reaches a maximum and then decreases at higher vanadia loadings. Previous studies of the activity of vanadia doped carbon-based catalysts, conducted at lower temperatures, have also shown an increase in the rate of the SCR reaction with vanadia loadings [19]. NO conversion at 150 °C in the presence of no V loading catalysts reaches a value lower than 8% [36].

Among possible causes, this increase could be due to the change in the V oxidation, textural and chemistry properties of the catalysts. Similarly this increase of SCR activity as long as vanadia loading increases to a certain extent has also been observed in metal-oxide based catalysts. In 1996 Amaridis [20] reported the turnover frequency of the V₂O₅/TiO₂ catalysts reached a maximum at a coverage corresponding to approximately half a monolayer, and then decreases at higher coverages. Such an increase has been attributed to a higher specific activity of the polymeric vana-

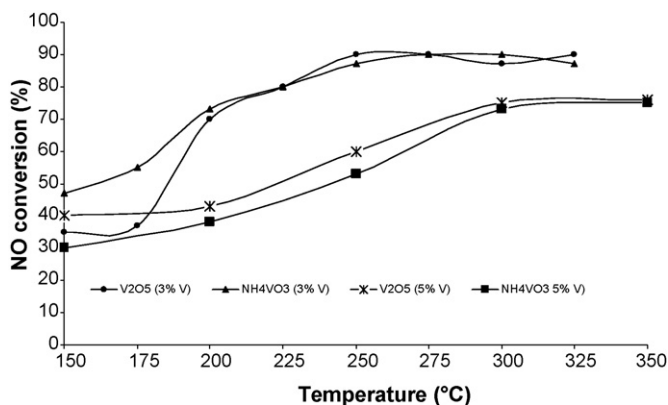


Fig. 2. Activity of 3 and 5% of vanadia loaded catalysts from two different precursors.

Table 2

Textural characterization of carbon-based catalysts with different vanadia loadings.

Active phase precursor and loading	Textural characterization					D_p (Å)
	S_{BET} (m ² /g)	$V_{\text{micropore } <0.7 \text{ nm}}$ (cc/g)	$V_{\text{micropore media}}$ (cc/g)	$V_{\text{micropore total}}$ (cc/g)	V_{BHJ} (cc/g)	
Support	651	0.0120	0.0052	0.0172	0.0330	65
NH ₄ VO ₃ (1%V)	559	0.0185	0.0071	0.0255	0.0165	78
NH ₄ VO ₃ (3%V)	570	0.0088	0.0039	0.0128	0.0263	87
NH ₄ VO ₃ (5%V)	486	0.0039	0.0031	0.0070	0.0272	99
V ₂ O ₅ (1%V)	515	0.0050	0.0094	0.0144	0.0528	63
V ₂ O ₅ (3%V)	445	0.0090	0.0058	0.0148	0.0460	83
V ₂ O ₅ (5%V)	490	0.0087	0.0069	0.0157	0.0494	78

date species [21], or the accompanying increase of Brønsted acid sites with vanadia surface coverage [22]. The lower turnover frequency observed at coverages exceeding one monolayer are due to the presence of microcrystalline V₂O₅ particles which are not 100% dispersed as assumed in the turnover frequency calculations. The observed maximum, and the subsequent decrease of the SCR turnover frequency at coverages between half and one monolayer can be attributed to the loss of strong acid sites at high vanadia surface coverages. Acid sites are expected to be involved in the adsorption and subsequent activation of NH₃ for the SCR reaction.

Moreover, Fig. 2 shows the activity of 3 and 5% of vanadia loading catalysts from different precursors in the whole range of studied temperature (150–350 °C). As seen, 3% doped catalysts show a higher activity, especially at medium temperatures. This fact can be related to the vanadia morphology.

There are several techniques to characterize the presence of vanadia on the surface catalysts. Those that are available in our laboratories have been used in this work. In this work textural and chemistry characterization has been carried out. To investigate the effect of V loading on textural and catalytic properties of the catalyst, three different loadings of V from two different active phase precursors have been prepared. Table 2 shows the surface area (S_{BET}), the pore volume (V_p) and the mean pore diameter (D_p) obtained from the experimental pore size distribution.

The surface area decreases after vanadia impregnation in all cases. The mean pore diameter increases and the pore volume decreases as long as vanadia loading increases. For non-doped carbon-based support a surface area of 650 m²/g is exhibited while after impregnation surface area is reduced around 32 and 12% depending on vanadia loadings. The increase of the mean diameter pore after impregnation is also noticeable. The higher the vanadia loading is, the higher the mean diameter is. Both facts point out that vanadia deposition occurs on the entrance of small pores blocking them.

The vanadia surface coverage has been calculated taking into account that the nominal VO_x surface density at monolayer coverage of our carbon is 1.16 Vnm⁻² and therefore resulting at monolayer coverage a value of 1.19 mmol/g (around 6 wt% V of carbon coating) [30]. Although the maximum vanadia loading used in this work does not reach this theoretical value, vanadia seems to be present as V₂O₅ crystallines particles because of the activity

Table 3V⁴⁺/V⁵⁺ ratio for carbon-based catalysts detected by XPS.

Vanadia loading (NH ₄ VO ₃)	Deconvolution of V _{2p} peak	
	BE (eV)	V ⁴⁺ /V ⁵⁺
1 wt%	515.5	1.42
	517.2	
3 wt%	515.9	3.42
	517.4	
5 wt%	516.0	0.28
	517.2	

tests and previous characterization. Previous studies have shown that depending on the vanadia loading, two surface vanadia species and microcrystalline phase V₂O₅ particles can be present on the surface of V₂O₅/AC catalyst [23]. In brief, at low vanadia loadings vanadia exists on the carbon surface primarily as an isolated, tetrahedrally coordinated, surface vanadyl species, with a valence of V⁴⁺. At higher vanadia loadings, the surface vanadyl species polymerise on the carbon surface. At coverage exceeding a monolayer, microcrystalline V₂O₅ particles are formed as a separate phase on the two-dimensional surface vanadia over layer, vanadia valence corresponds to V⁵⁺.

XPS runs were carried out to determine the valence state of vanadia depending on vanadia loadings. Table 3 shows V⁴⁺/V⁵⁺ ratios obtained showing a maximum of V⁴⁺ concentration when vanadia loading reached 3 wt%. Moreover, the valence state of vanadia depends on the functionalities present on carbon surface and consequently the study of C_{1s} peak can provide valuable information (see Table 4). Vanadia loading of 3 wt% has the maximum graphitic content. According to these tables, the oxidation state of vanadia apparently not only depends on the vanadia loading but also on the functionalization of carbon.

Catalyst activity research is still in progress. Actually, stability of catalyst under higher temperatures and longer operation times is been investigated showing that they are stable up to 400 °C with a stable NO conversion. Further results are expected to be reported in following works.

3.2. Effect of tungsten loading

The influence of a second active phase presence on the SCR catalytic activity was tested by the impregnation with tungsten. W impregnation was carried out with 5 wt% by ionic exchange impregnation in the same holder as vanadia impregnation. Results are reported in Fig. 3.

As reported in literature [24], it has been observed that the reactivity of commercial catalysts, mostly based on metal oxides, in the SCR reaction is increased by either increasing vanadia or

Table 4Deconvolution of C_{1s} peak from XPS data of vanadia doped carbon-based catalysts.

Vanadia loading (NH ₄ VO ₃)	BE (eV)	Relative amount (%)	Carbon assignation
1 wt%	284.7	69	C-graphitic
	286.4	18	C-phenolic-ether
	288.5	8	C-carbonylic
	290.7	5	C-carboxylic
3 wt%	284.8	73	C-graphitic
	286.4	16	C-phenolic-ether
	288.7	7	C-carbonylic
	290.8	4	C-carboxylic
5 wt%	284.7	61	C-graphitic
	286.3	22	C-phenolic-ether
	288.7	11	C-carbonylic
	290.8	6	C-carboxylic

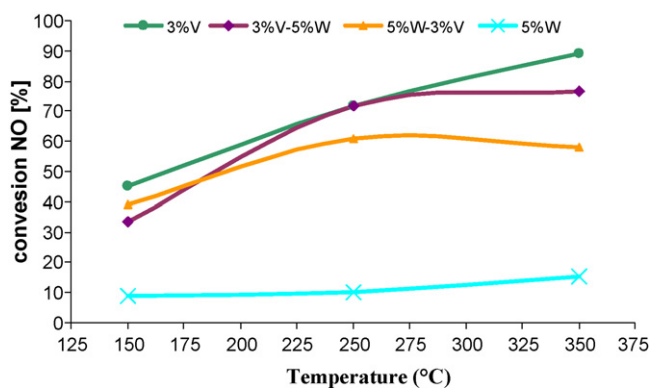


Fig. 3. Activity of tungsten loaded catalysts.

tungsten loadings, because of higher NO conversions achieved at lower temperatures. This fact is due to the decrease of both the temperature of the onset of the SCR reaction (T_{SCR}) and the catalyst reoxidation temperature (T_{OX}) thanks to either by increasing the V and/or W loading [25]. The temperature decrease could be due to an increase of the redox properties of the catalyst samples, being T_{SCR} and T_{OX} indicative of the catalyst reduction processes, respectively. Another factor that can affect SCR activity when W is doped as a second active phase in commercial catalysts is the formation of new Brönsted acid sites [26], because of the requirement of a dual-site mechanism for the SCR reaction [27] or an acid and redox catalyst function [28].

However, those carbon-based catalysts impregnated with W after, before or simultaneously as V impregnation do not show any enhancement of catalytic activity. More in detail, catalysts firstly impregnated with V and subsequently with W present a higher activity than those with the impregnation order in the other way round or even those which have been simultaneously impregnated. This fact could be explained by invoking different factors.

According to other authors [4,5], and as commented previously, tungsten addition provides a higher acid site density. Consequently, carbon-based catalyst impregnation with W can provide the creation of new Lewis acid sites that avoid a proper distribution and anchoring of V on catalysts surface. Although a moderate increase of surface acidity improves NH_3 adsorption, a too high acidification of

surface does not allowed NH_3 desorption and consequently avoids it to take part in the SCR reaction. TPD- NH_3 runs were carried out in all cases to determine the total acidity and point out roughly the amount and type of new acid sites created after impregnation. NH_3 desorption is not a quantitative technique but it can give a roughly impression of the acid site distribution on catalysts surface. Table 5 reports the data. As shown the presence of Brönsted sites are only observed in just vanadia loaded catalysts or simultaneous vanadia and tungsten loaded catalysts. In addition, the impregnation with W shifts NH_3 desorption from lower temperatures that are mainly corresponding to Brönsted acid centres towards higher temperatures indicating a higher strength of the bond.

TPD- NH_3 could be related to the catalytic activity since just vanadia loaded catalysts present the highest activity in the whole range of temperatures and just tungsten loaded catalysts the lowest activity what nicely agrees to other authors who suggest that Brönsted sites promote SCR activity [4,5].

Another factor for the lower NO activity is that tungsten impregnation can reduce textural properties of supports in a similar way to that observed for vanadia impregnation making difficult a good dispersion of vanadia on the surface in the following step. Textural characterization was carried out by means of N_2 isotherms at $-196^\circ C$ and results are reported in Table 6.

As observed all catalysts show a similar textural characterization. Surface area, volume pore and mean diameter of just vanadia doped catalyst and any other catalysts are really close. This fact points out that the decrease in activity is not due to a pore blocking. Taking into account the characterization previously exposed we can suggest that the decrease of activity is mainly due to a change in the chemistry surface.

It has been proposed that V and W species on commercial catalysts are primarily in the form of surface vanadyls and wolframyls with one short V=O and W=O bond, respectively, and that their primary interaction is with the TiO_2 support [26]. So, the active phase is V, although V and W centres can interact electronically each other through the TiO_2 semiconductor support. NO consumption is principally ascribed to the presence of vanadium only, whereas Ti-sites as well as V- and W-oxide species act as adsorption sites for ammonia. Accordingly these species act as ammonia “reservoir” or “storage”. This NH_3 storage can be involved in the SCR reaction upon “migration” to near-by reactive V-sites where NH_3 is consumed by gas-phase NO [5]. As carbon is not a semiconductor material, it is really unlikely that this interaction between V- and W-oxide species

Table 5
TPD- NH_3 of binary carbon-based catalysts.

Catalysts	Q_{NH_3} (mmol/g)	Brönsted sites		Lewis sites	
		T (°C)	Q_{NH_3} (mmol/g)	T (°C)	Q_{NH_3} (mmol/g)
NH_4VO_3 (3% V)	0.2306	176	0.0028	563	0.2278
5% W	0.0370			571	0.0370
3% V–5% W	0.0625			485	0.0625
5% W–3% V	0.1002			519	0.1002
3% V–5% W simultaneously	0.0993	206	0.0053	600	0.0940

Table 6
Textural characterization of carbon-based catalysts with different vanadia loadings.

Active phase precursor and loading	Textural characterization					
	S_{BET} (m^2/g)	$V_{micropore < 0.7 nm}$ (cc/g)	$V_{micropore media}$ (cc/g)	$V_{micropore total}$ (cc/g)	V_{BHJ} (cc/g)	D_p (Å)
NH_4VO_3 (3% V)	407	0.0151	0.0050	0.0202	0.0276	68
5% W	451	0.0150	0.0044	0.0214	0.0218	65
3% V–5% W	486	0.0157	0.0046	0.0223	0.0233	60
5% W–3% V	503	0.0150	0.0069	0.0218	0.0225	59

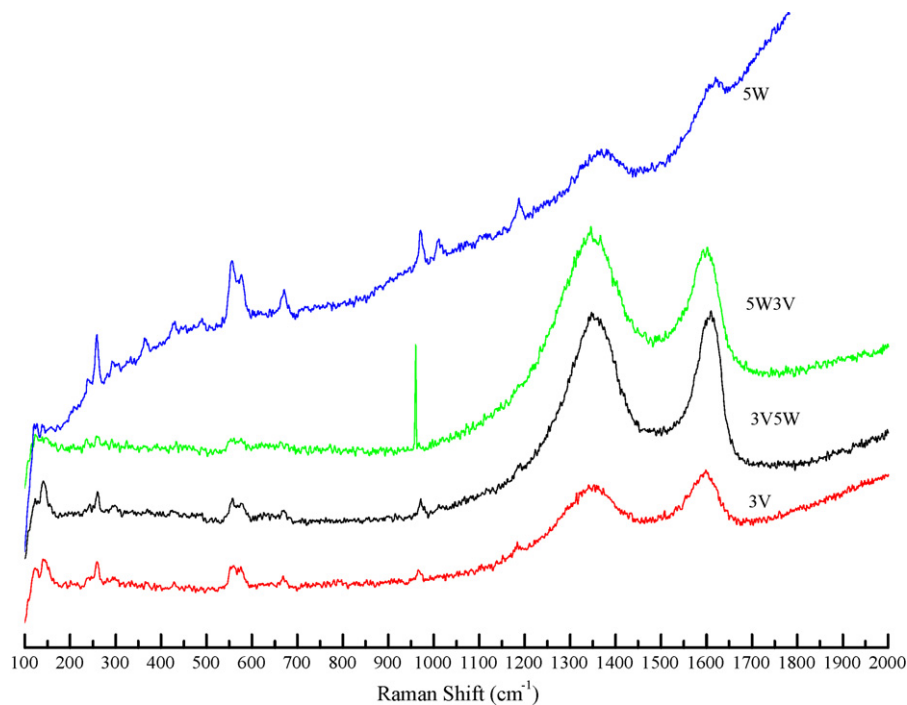


Fig. 4. Raman spectra (2× magnified) of vanadia–tungsten loaded catalysts in the 100–2000 cm⁻¹ region.

can take place in. Moreover, the reactivity of V being roughly 6 times higher than that of W makes binary impregnation to get poor active catalysts.

These results agree to those presented by Zhu et al. [29] and García-Bordejé et al. [30]. Zhu et al. observed a decrease of SCR activity of carbon-based catalysts doped with vanadia and tungsten almost negligible in the range of low temperatures that was ascribed to higher acidity of Brønsted centres that avoiding a proper NH₃ desorption.

Fig. 4 shows the Raman spectra in the area of the 100–2000 cm⁻¹. Main crystal lattice vibration of cordierite (128, 260, 555, 578, 973, 1011, 1382 cm⁻¹) are presented in all spectra.

Besides, the two typical signals of the carbon structure at 1340 and 1592 cm⁻¹ are detected. The first signal is assigned to defect mode, A_{1g} (signal D) and the second is associated with graphite, mode E_{2g} (signal G). The integrated intensity ratio of these two signals, D and G, in the Raman spectrum is related to graphite crystallite size (L_n) according to [31]:

$$L_n \text{ (nm)} = \frac{4.4}{R} \quad \text{where } R = \frac{I_D}{I_G} \quad (3)$$

Considering that both signals have similar extinction coefficients, it is possible to get the graphitic fraction according to:

$$X_G = \frac{I_G}{I_G + I_D} = \frac{1}{1 + R} \quad (4)$$

The values of the graphitic fraction (X_G) for these catalysts obtained in our studies are between 0.23 and 0.38. In Table 7 is resumed all these parameters.

Table 7
Resume of carbon coating characterization parameters from Raman.

Active phase precursor and loading	I_D/I_G	L_n (nm)	X_G
Support	1.63	2.69	0.38
NH ₄ VO ₃ (3% V)	1.38	3.18	0.24
5% W	1.32	3.33	0.23
3% V–5% W	1.73	2.54	0.28
5% W–3% V	1.67	2.63	0.27

As shown in Raman spectrums, there is a clear presence of graphite and carbon as non-graphitic material. In order to go deeper in the distribution of these carbon materials and also how vanadium and tungsten are distributed over them, TEM runs have been performed.

Fig. 5 shows that only for the 5 wt% vanadium doped catalyst, the vanadium under V₂O₅ can be seen, confirmed with EDX. This fact means that the dispersion of vanadium as well as that of tungsten is really good. Unfortunately this technique does not relevant further information about the distribution of these metals onto the matrix. For this reason, catalyst characterization with MEV and LIBS techniques is proposed for following works.

Table 8
Resume of XPS data for carbon-based V–W loaded catalysts.

Peak area	5W3V	3V5W	5W	3V
C _{1s}	72.3	49.6	28.1	88.4
Al _{2p}	5.2	11.1	5.7	0.5
Si _{2p}	9.7	16.0	16.5	1.6
O _{1s}	12.8	23.2	49.7	9.5
W _{4f}	<0.5	<0.5	<0.5	–
V _{2p}	<0.5	<0.5	–	<0.5
Si/Al	1.8	1.4	2.9	3.1
C/O	5.6	1.8	0.6	9.3
V ⁴⁺ /V ⁵⁺	0.3	0.4	–	3.4

Table 9
V⁴⁺/V⁵⁺ ratio for carbon-based V–W loaded catalysts detected by XPS.

Catalyst	Deconvolution of V _{2p} peak	
	BE (eV)	V ⁴⁺ /V ⁵⁺
5W3V	514.8	0.3
	516.8	
3V5W	515.0	0.4
	517.1	
3V	515.9	3.4
	517.2	

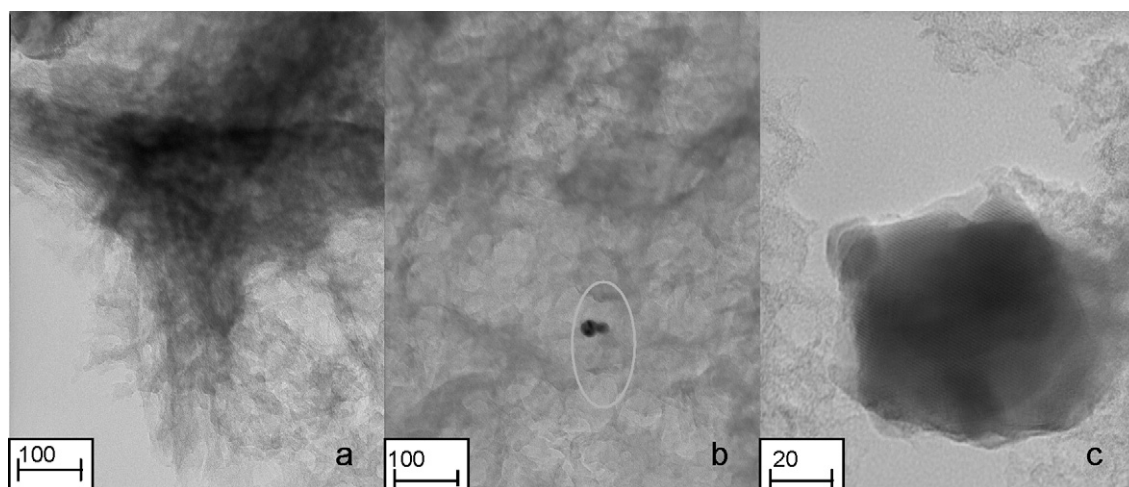


Fig. 5. TEM images of the 5% V doped catalyst.

In order to obtain a deeper knowledge of the surface properties of the as-prepared catalysts, XPS runs were performed and resumed in Tables 8 and 9. Al_{2p} , Si_{2p} and O_{1s} peaks are obtained with an average shift of around 4 eV, while C and metals deposited on it remain centred at their usual BE. This fact can point out that carbon is not a conductor material and consequently it avoids the appropriated transmission of the electronic beam. Moreover, it agrees with the proposal of other authors [24–26] that suggesting the avoidable electronic transmission between V and W atoms through the carbon coating and therefore the poor activity of this kind of bimetallic doped carbon-coated catalysts.

Going into further details, it must be said that although carbon coatings are really homogenous as reported previously in [32], it is observed a higher ratio Si/Al for the sample doped with just 5% of W, suggesting the possibility of having a XPS run from an area with a really thin carbon coating in comparison to the other XPS results. In addition the deconvolution of C_{1s} peak provides shifted peaks towards higher BE values, what confirms the interaction of ceramic material. The differences in coating thickness have to taken into account in the following comments as not all data are provided in the same conditions. Just on the contrary, sample doped with 5% of W and 3% of V provides a high C/O ratio which indicates the existence of a thicker carbon coating in this area.

According to W and V signals and their relation to C and O ones, it is observed that doping firstly with W and subsequently with V, the lowest V^{4+}/V^{5+} ratio is achieved. This fact agrees with the activity results reported above. What is remarkable about this fact is that doping firstly with W an important shift of V_{2p} peak takes place. This shift towards lower BE values indicates a lower V oxidation state approaching the BE that corresponds to V^{3+} and V^{4+} instead of V^{4+} and V^{5+} . The shift of V_{2p} peak towards lower BE values can agree (as well with the higher acidity character of these samples in comparison to V doped ones) with certain electronic density variation associated with metallic centres as well as disruption caused by the L_n values of graphitic species.

It is worth noting that the amount of W (for all catalysts, W is as W^{+6}) is almost depleted in all samples. This fact suggests the high dispersion of this metal through the surface since the total amount is much higher than that of V.

4. Conclusions

Combined chemical–physical and reactivity techniques have been used to test the characteristics of vanadia and tungsten loaded

carbon-based catalysts in the SCR reaction. The results presented above show that the state of vanadia is strongly dependent on loading and carbon functionalizations. Vanadia content strongly influences the catalytic behaviour: increasing vanadia loading leads to higher NO conversions to a certain extent and NO maximum conversions were observed at 3 wt% V.

Indeed the maximum in NO conversion seems to be related to the well dispersed and isolated vanadium oxide species detected as V^{4+} . Catalysts loaded with 3 wt% V shown the highest V^{4+}/V^{5+} whereas higher or lower vanadia loadings correspond to lower V^{4+}/V^{5+} ratios. Also the acidity of catalysts is changed due to the different V loading used. This fact could be pointed out as one of the reasons for increasing the NO conversion. Moreover, it has also been observed that crystallites of V_2O_5 are likely formed when its concentrations are greater than 5 wt% V. Although vanadia impregnation always causes a decrease of textural properties, vanadia loadings from 5 wt% on show a remarkable porosity loss, especially in micropore volume pointing out the existence of crystallines at the pore entrance.

Tungsten impregnation was carried out after, before and simultaneously to vanadia impregnation. On the contrary to commercial SCR catalysts, there were no signs of catalytic enhancement due to the presence of tungsten onto catalyst surface. This fact can be due to either an acidification of surface that does not allow a proper NH_3 desorption avoiding it to take part in the SCR reaction or a poor electronic interaction between carbon and V and W oxides that does not improve the redox properties resulting in both cases in a decrease of SCR activity.

Acknowledgements

This research was financed by the project 437/2006/13.1 and B34/2007 (Ministerio de Medio Ambiente, Spain) and by the project CTQ2006-09870 (Ministerio de Educación y Ciencia, Spain). A. Boyano wants to thank CSIC for her I3P predoctoral grant.

References

- [1] A. Cybulski, J.A. Moulijn, Structurated Catalysts and Reactors, Taylor, 2006.
- [2] C. Ciardelli, I. Nova, E. Tronconi, B. Konrad, D. Chartterjee, K. Ecke, M. Weibel, Chem. Eng. Sci. 59 (2004) 5301–5309.
- [3] J.W. Choung, I.S. Nam, S.E. Ham, Catal. Today 111 (2006) 242–247.
- [4] H. Bosch, F. Janssen, Catal. Today 2 (1988) 369.
- [5] P. Forzatti, L. Lietti, Heter. Chem. Rev. 3 (1996) 33.
- [6] A. Baiker, P. Dollenmeier, M. Clinski, Appl. Catal. 35 (1987) 351.
- [7] J.P. Chen, R.T. Yang, Appl. Catal. A 80 (1992) 135–148.

- [8] G. Connell, J.A. Dumesic, *J. Catal.* 105 (1988) 38.
- [9] T. Yamaguchi, Y. Tanaka, K. Tanabe, *J. Catal.* 65 (1980) 442.
- [10] P.A. Burke, E.I. Ko, *J. Catal.* 129 (1991) 38.
- [11] Z. Huang, Z. Zhu, Z. Liu, *Appl. Catal. B: Environ.* 39 (2002) 361–368.
- [12] A. Boyano, M.E. Gálvez, M.J. Lázaro, R. Moliner, *Carbon* 44 (2006) 2399.
- [13] E. García-Bordejé, L. Calvillo, M.J. Lázaro, R. Moliner, *Appl. Catal. B: Environ.* 50 (2004) 235.
- [14] E. García-Bordejé, M.J. Lázaro, R. Moliner, P.M. Álvarez, V. Gómez-Serrano, J.L.G. Fierro, *Carbon* 44 (2006) 407–417.
- [15] Q.L. Zhuang, T. Kyotani, A. Tomita, *Energy Fuels* 8 (1994) 714–718.
- [16] J.L. Figueiredo, M.F.R. Pereira, M.M.A. Freitas, J.J.M. Orfao, *Carbon* 37 (1999) 1379–1389.
- [17] H.P. Boehm, *Carbon* 32 (1994) 759–769.
- [18] M.V. Lopez-Ramón, F. Stoeckli, C. Moreno-Castilla, F. Carrasco-Marin, *Carbon* 37 (1999) 1215–1221.
- [19] V.I. Marshneva, E.M. Slavinska, O.V. Kalinkina, G.V. Odegova, E.M. Moroz, G.V. Lavrova, A.N. Salanov, *J. Catal.* 155 (1995) 171.
- [20] M.D. Amiridis, I.E. Wachs, G. Deo, J.M. Jehng, D.S. Kim, *J. Catal.* 161 (1996) 247–253.
- [21] G.T. Went, L.J. Len, R.R. Rosin, A.T. Bell, *J. Catal.* 134 (1992) 492.
- [22] N.Y. Topsoe, H. Topsoe, J.A. Dumesic, *J. Catal.* 151 (1995) 226.
- [23] U.S. Ozkan, Y. Cai, M.W. Kumthekar, *J. Phys. Chem.* 99 (1995) 2363.
- [24] L. Lietti, G. Ramis, F. Berti, G. Toledo, D. Robba, G. Busca, P. Forzatti, *Catal. Today* 42 (1998) 101–116.
- [25] L. Lietti, P. Forzatti, *Appl. Catal. Lett.* 41 (1996) 35.
- [26] L.J. Alemany, L. Lietti, N. Ferlazzo, P. Forzatti, G. Busca, G. Ramis, E. Giamello, F. Bregani, *J. Catal.* 117 (1995) 155.
- [27] I.E. Wachs, G. Deo, B.M. Weckhuysen, A. Andrini, M.A. Vuurman, M. de Boer, M.D. Amiridis, *J. Catal.* 161 (1996) 211.
- [28] M.C. Paganini, L. Dell'Acqua, E. Giamello, L. Lietti, P. Forzatti, G. Busca, *J. Catal.* 166 (1997) 195.
- [29] Z. Zhu, Z. Liu, S. Liu, S.H. Niu, *Appl. Catal. B: Environ.* 30 (2001) 267–276.
- [30] E. García-Bordejé, M.J. Lázaro, R. Moliner, J.F. Galindo, J. Sostres, A.M. Baro, *Appl. Catal. B: Environ.* 228 (2004) 135–142.
- [31] M.A. Ulla, A. Valera, T. Ubieto, N. Latorre, E. Romeo, V.G. Milt, A. Monzón, *Catal. Today* 133–135 (2008) 7–12.
- [32] A. Boyano, M.J. Lázaro, C. Cristiani, F.J. Maldonado-Hodar, P. Forzatti, R. Moliner, *Chem. Eng. J.* 149 (2009) 173–182.
- [33] M. Koebel, M. Elsener, M. Kleeman, *Catal. Today* 59 (2000) 335.
- [34] E. García-Bordejé, M.J. Lázaro, R. Moliner, *J. Catal.* 223 (2004) 395–403.
- [35] A. Boyano, M.E. Galvez, R. Moliner, M.J. Lázaro, *Fuel* 87 (2008) 2058–2068.
- [36] L. Calvillo, E. García-Bordejé, M.J. Lázaro, Final Thesis Diplome, University of Zaragoza, Spain, 2003.